Detailed Chemical Kinetics Study of the Role of Pressure in Butane Pyrolysis

Richard G. Mallinson*
School of Chemical Engineering and Materials Science, The University of Oklahoma, Norman, Oklahoma 73019

Robert L. Braun, Charles K. Westbrook, and Alan K. Burnham
Lawrence Livermore National Laboratory, L-207, P.O. Box 808, Livermore, California 94551

A detailed free-radical kinetic model has been developed to represent the pyrolysis of *n*-butane and has been used to study the role of pressure on the pyrolysis. The temperature range covered is from 200 to 600 °C with pressures from 1 to 1000 atm. Simulations were conducted for isothermal, isobaric, homogeneous systems with pure *n*-butane as the initial reactant. At high temperature, increasing the pressure increases the decomposition rate of butane, as well as increasing the breadth of the carbon number distribution and decreasing the olefins content. Model results agree well with the literature. At low temperature, the rate of decomposition of butane is inhibited by increasing pressures until relatively high pressures, above 100 atm, when the rate increases with higher pressures. Increased pressures at lower temperatures also favor larger products and fewer olefins, but different mechanistic pathways control the decomposition.

Introduction

Hydrocarbon pyrolysis has been the subject of significant study since the early days of petroleum processing. The primary technical application to this area has led to a focus of research on conditions of relatively high temperatures, above 500 °C, and pressures near atmospheric. This is the region in which thermal cracking of light alkanes is used to produce olefins such as ethylene and propylene. The conditions of interest in the present work are those under which the geologic maturation of petro-

0888-5885/92/2631-0037$03.00/0

leum occurs, with temperatures at or below about 200 °C and pressures up to 1000 atm and higher. In order to understand the role of pressure in hydrocarbon pyrolysis, a detailed chemical reaction model has been formulated and computer simulations have been carried out, both at conditions where extensive research has been previously conducted and at conditions of geochemical interest. The solutions at relatively high temperature, 600 °C, and atmospheric pressure have been obtained in order to evaluate the results in a region where there is a significant knowledge base with which to judge them. As one approaches lower temperatures, there is little evidence to provide any significant evaluation.

The initial development of an understanding of hydrocarbon cracking, indeed of chain reactions, is attributable to the work of Rice and Herzfeld (1934) and Kossiakoff and Rice (1943). They identified the chain steps for radical reactions as initiation, termination by recombination and disproportionation, hydrogen transfer, addition, decomposition, and isomerization. Their analyses examined the statistics and energetics of the reactions in sufficient detail to allow estimation of product distributions. Experimentally, Voge and Good (1949) demonstrated the validity of these product distributions at atmospheric pressure and observed the effect of elevated pressures, up to 21 atm, on the product distributions. At atmospheric pressure, primarily light olefins are found from cracking *n*-hexadecane at 500 °C with no paraffins larger than ethane present. At elevated pressures, they found that the average molecular weight of the products increased and paraffins of larger sizes were present. Additionally, they found that the rate of decomposition of *n*-hexadecane increased significantly. These qualitative findings have been confirmed in other experimental studies over the years, and a substantial review of the early cracking literature was conducted by Fabuss et al. (1964) from which these conclusions are confirmed, although they indicate that some studies show little effect of pressure on the rate of cracking over relatively limited ranges of pressure.

There are few data at pressures above about 100 atm. Gonikberg et al. (1953) studied hexane and heptane cracking at temperatures around 420 °C and pressures between 100 and 3100 atm, but these data were obtained in such a way as to make general conclusions difficult. Hepp and Frey (1953) studied the pyrolysis of butanes and of propane at pressures of 100 and 170 atm at temperatures between 520 and 550 °C in a tubular flow reactor. Their experiments with *n*-butane used residence times sufficient to give butane conversions from 11 to 62%. They did not observe a significant difference between the butane decomposition rate at 100 and 170 atm, although their temperature and pressure varied somewhat from experiment to experiment. (They did find that the rate of decomposition of isobutane was retarded by the increase in pressure.) Detailed data on product distributions indicated that the olefins content was decreased and production of heavier products was increased at higher pressure. Of significant interest is the recent work of Dominé (Dominé, 1989, 1991; Dominé et al., 1990). That work had a goal quite similar to that of this paper, that is, understanding the role of pressure on the thermal transformations of petroleum by looking at the pyrolysis of hydrocarbons. Of particular interest to the present work was their study of the pyrolysis of *n*-hexane at pressures from 210 to 15 600 atm at 357 °C and for several additional temperatures, from 290 to 365 °C, at one pressure, 210 atm. The temperatures used, lower than other studies at high pressures, are particularly useful for providing insights into the low-temperature-pyrolysis behavior of interest in petroleum maturation with the limitation, however, of low conversions, less than about 2% of the initial *n*-hexane. A free-radical kinetic model was proposed, for which the results agreed well with the data. The consideration of only low-conversion behavior allowed considerable simplification of the model due to the dominance of the *n*-hexyl radicals in the system. Their model, in addition to using an equation of state to estimate the density of the system, used estimates for the activation volumes for the reaction rate parameters to account for the pressure dependence of those parameters. Among their significant conclusions were that the gas-phase rate parameters were able to represent the system quite well and that the rate of decomposition of *n*-hexane decreased with increasing pressure, and this dependence became larger with lower temperature, in contradiction to previous high-temperature studies (Fabuss et al., 1964; Doue and Guiochon, 1968). Mechanistically, Dominé et al. proposed that, at higher temperatures and lower pressures, the system is dominated by decomposition reactions, while, at lower temperatures and higher pressures, hydrogen-transfer reactions dominate the system. The present study confirms the conclusions of Dominé (Dominé et al., 1990) concerning the complex interactions between the effects of temperature and pressure, but we have carried out the system evaluation to much greater extents of conversion with a considerably more detailed mechanism, thereby obtaining additional information and insight into the dominant reaction pathways.

Reaction Mechanism

The reaction mechanism of this study for butane pyrolysis has as its origins the hydrocarbon oxidation model developed by Westbrook et al. (Axelsson et al., 1986; Westbrook et al., 1988). The present model began as a hydrocarbon reaction subset of that oxidation model but has since undergone extensive modification.

The model consists of 209 chemical species and 945 elementary reactions with forward and reverse rate constants defined for each reaction. The model is a fairly comprehensive representation of chemically feasible reactions. It includes appropriate initiation–termination reactions, radical-transfer reactions, addition–decomposition reactions, and alkyl isomerization reactions for noncyclic species containing from one through seven carbons along with hydrogen. One significant assumption, however, is that hydrogen abstraction from the large alkane species occurs only by H, CH_3, C_2H_5, and C_3H_7 radicals, which are the predominant radical species in this system. These abstraction reactions can be expressed collectively as

$$RH + (H, CH_3, C_2H_5, C_3H_7) = R + (H_2, CH_4, C_2H_6, C_3H_8)$$

where R represents an alkyl radical. A related assumption is that these abstraction reactions produce the appropriate distribution of large radical types, thereby precluding the need for abstraction reactions by larger alkyl radicals. Alkyl radicals larger than ethyl are assumed to decompose thermally to produce an olefin and a smaller alkyl radical, to add to olefins to produce larger alkyl radicals, or to recombine with other alkyl species to produce larger alkane species. The reverse of the abstraction reaction provides another path for production of alkanes larger than the initial reactant species.

One aspect of the model is more limited, and this encompasses cyclization reactions to form cyclopentyl and cyclohexyl species. The extensive presence of cycloalkanes

and aromatics in petroleum suggests that they must be included in any attempt to understand the chemical reactions involved in petroleum maturation. However, as opposed to that for noncyclic species, the available knowledge base for thermal reactions of cyclic species is considerably more limited and provides the difficult choice of inclusion of reactions and rate parameters subject to considerably more uncertainty than those for noncyclics or consideration of a simplified mechanism to represent their behavior. In this research, the latter choice was made, and the basis was provided from the work of Ebert et al. (1983). These species are assumed to be formed only by cyclization of 5, 6, and 7 carbon dienyl species. Once formed, the cyclic species may undergo only hydrogenation–dehydrogenation reactions to form stable cycloalkanes or cycloolefins, including benzene and toluene.

Because of the large number of species and reactions, it is not feasible to present the model in its entirety. (A complete listing of the species, reactions, and rate parameters is available from the authors.) However, so that the structure of the model may be understood, the reactions involving one isomer of heptane and its derivatives will be presented in an abbreviated format. As is easily understood, as the number of carbon atoms in the hydrocarbon increases, the number of isomers and reactions increase dramatically. For example, the model includes eight nonlinear isomers of heptane (C_7H_{16}), and the incorporation of the reactions related to these isomers accounts for 381 of the 945 reactions in the model. While there are fewer species and fewer reactions as the number of carbons decrease, there are also, in some cases, additional reactions and species not covered in this example. For example, the C_7 reactions do not include formation of diolefins, while for smaller species such reactions are included. Reactions forming butadiene and acetylene are two examples of these:

$$iC_5H_9 = C_4H_6 + CH_3$$

$$C_2H_3 + CH_3 = C_2H_2 + CH_4$$

The reactions related to 2-methylhexane (denoted $2C_7H_{16}$) are selected as an example. For clarity, the backbone carbons are identified by letters which carry through to identify radicals and other seven-carbon derivatives:

$$\begin{array}{c} CH_3 \\ CH_3CHCH_2CH_2CH_2CH_3 \\ a\ \ b\ \ c\ \ d\ \ e\ \ f \end{array}$$

There are eleven initiation–termination reactions for this species. Six C_7H_{15} radicals are produced:

$$2C_7H_{16} = aC_7H_{15} + H$$

$$2C_7H_{16} = bC_7H_{15} + H$$

$$2C_7H_{16} = cC_7H_{15} + H$$

$$2C_7H_{16} = dC_7H_{15} + H$$

$$2C_7H_{16} = eC_7H_{15} + H$$

$$2C_7H_{16} = fC_7H_{15} + H$$

One reaction produces a five-carbon fragment:

$$2C_7H_{16} = dC_5H_{11} + C_2H_5$$

Where dC_5H_{11} is the 2-methyl-4-butyl radical. Two reactions result in six-carbon fragments:

$$2C_7H_{16} = 2C_6H_{13} + CH_3$$

$$2C_7H_{16} = eC_6H_{13} + CH_3$$

where $2C_6H_{13}$ is the 2-hexyl radical and eC_6H_{13} is the 2-methyl-5-pentyl radical. Lastly, three- and four-carbon fragments are formed via two reactions:

$$2C_7H_{16} = iC_3H_7 + pC_4H_9$$

$$2C_7H_{16} = iC_4H_9 + nC_3H_7$$

Radical transfer by hydrogen abstraction from H, CH_3, C_2H_5, and C_3H_7 each produce the six C_7H_{15} radicals, a–f, as illustrated by those producing aC_7H_{15}:

$$2C_7H_{16} + H = aC_7H_{15} + H_2$$

$$2C_7H_{16} + CH_3 = aC_7H_{15} + CH_4$$

$$2C_7H_{16} + C_2H_5 = aC_7H_{15} + C_2H_6$$

$$2C_7H_{16} + C_3H_7 = aC_7H_{15} + C_3H_8$$

The six C_7H_{15} radicals can isomerize via internal H abstraction, with the a radical able to isomerize to the d, e, and f radicals; the b to the e and f radicals; and the c radical to the f radical. For example

$$aC_7H_{15} = eC_7H_{15}$$

Decomposition of the six C_7H_{15} radicals (and inversely, addition to produce them) requires nineteen reactions. For example, aC_7H_{15} decomposes in three ways:

$$aC_7H_{15} = C_3H_6 + pC_4H_9$$

$$aC_7H_{15} = 1C_6H_{12} + CH_3$$

$$aC_7H_{15} = aC_7H_{14} + H$$

where $1C_6H_{12}$ is the linear α-olefin, 1-hexene, and aC_7H_{14} is 2-methyl-1-hexene. The b- and eC_7H_{15} also have three decomposition reactions while the c and d isomers have four and the f isomer has two. The dominant decomposition path for aC_7H_{15} (i.e. with the lowest activation energy barrier) is the first listed above, producing C_3H_6 and the primary butyl radical via β-scission of the alkyl radical.

The decomposition reactions discussed above produce five possible olefins, designated a–eC_7H_{14}. Hydrogen-transfer reactions are included, but only with H and CH_3. For example

$$aC_7H_{14} + H = aC_7H_{13} + H_2$$

$$aC_7H_{14} + CH_3 = aC_7H_{13} + CH_4$$

The C_7H_{14} olefins may also decompose to form smaller fragments:

$$aC_7H_{14} = iC_4H_7 + nC_3H_7$$

$$bC_7H_{14} = C_2H_5 + iC_5H_9$$

$$cC_7H_{14} = CH_3 + iC_6H_{11}$$

$$dC_7H_{14} = iC_3H_7 + pC_4H_7$$

$$eC_7H_{14} = C_3H_5 + iC_4H_9$$

At this point, the model becomes degenerate in that only one C_7H_{13} radical is produced from all of the olefins, designated aC_7H_{13}. The aC_7H_{13} radical may decompose:

$$aC_7H_{13} = iC_4H_7 + C_3H_6$$

$$aC_7H_{13} = C_3H_5 + 1C_4H_8$$

$$aC_7H_{13} = pC_4H_7 + C_3H_6$$

$$aC_7H_{13} = C_3H_5 + iC_4H_8$$

As previously noted, decomposition to form C_7H_{12} diolefins does not take place, although such reactions are included for smaller (fewer carbons) olefinic radicals.

Rate Parameters

Rate parameter estimates are substantially those from the compilation of Allara and Shaw (1980). Where not

specifically available, parameters were estimated by extrapolation from analogous reactions with alterations appropriate for the thermochemical differences of the species. These differences were obtained from Stull et al. (1987) or by the estimation methods of Benson (1976). Reverse reaction rate parameters were obtained in several ways. For those reactions where equilibrium constants were available or could be calculated, reverse rate expressions were computed from the forward rate and the equilibrium constant. In other cases, reverse rate expressions were estimated in the same manner as the forward rate expressions described above. The parameters were of the Arrhenius form and included no explicit dependence on pressure. Pressure (or density) dependence is possible at either very low or very high pressures for various reasons. At very low pressures, reaction rates decrease for small molecules because collisions are not frequent enough to redistribute energy into all vibrational modes. All pressures considered in this study are higher than where this effect is important, so all reactions are considered to be at their "high-pressure" limit. At very high pressures, reaction rates can decrease due to changes in the thermodynamic stability of an activated-complex intermediate as well as cage and diffusional effects. Although there are models that account for such effects (cf. Asano and Le Noble, 1978), data and estimation methods for the reactions and conditions of this study are very limited. Dominé (Dominé et al., 1990) did include an activation volume dependence in his model studies, using nominal estimation of the activation volumes, but also noted that there was not a strong basis for their estimation. We have chosen to neglect this factor until it can be addressed more thoroughly. We do expect that increased pressures would be more inhibiting at all temperatures if activation volumes were included.

Computation

The solutions to the differential equations of this kinetic model were made using the CHEMKIN-II chemical kinetics package (Kee et al., 1989). This set of Fortran subroutines was compiled and executed on Sun 4 and Sun Sparcstation 1 workstations with 8 Mbyte of memory in both cases. An application code written for this package named SENKIN (Lutz et al., 1989) was found to execute the problems most quickly and provided the additional benefits of solving for the sensitivity coefficients for the system if desired. It also allowed problems to be restarted at intermediate points in previously solved problems. (This was convenient if more frequent output was desired or if sensitivities were desired at particular times of solution, which was of great computational time savings.) The SENKIN code was based upon the ODE sensitivity solution package developed by Caracotsios and Stewart (1985).

The CHEMKIN-II package was developed for solution of gas-phase kinetics problems, and it uses the ideal gas equation to calculate densities and therefore has a direct influence on the concentrations and reaction rates. At elevated pressures, the use of the ideal gas equation is inappropriate, and an equation of state is required to properly represent the density of the system. For this study, a highly accurate equation for calculation of the density correction was used (Starling and Kumar, 1985). In this form, the compressibility factor for the mixture is computed and used to correct the ideal gas density. The compressibility factor is defined as

$$Z = PV/nRT \quad (1)$$

The compressibility factor, Z, is equal to 1 for an ideal gas.

Table I. Comparison of Simulation Results with the Data of Hepp and Frey (1953) at 550 °C and 160 atm (ca. 57 wt % Conversion)

	Hepp and Frey data	SENKIN simulation[a]
reaction time/s	132	75
H_2	0.06	0.003
CH_4	10.48	7.1
C_2H_4	0.7	0.4
C_2H_6	10.19	4.9
C_3H_6	4.7	2.4
C_3H_8	6.27	6.1
C_4H_8	2.33	5.9
C_4H_{10}	43.02	43.8
pentenes	1.99	3.3
pentanes	2.65	1
hexenes	1.31	3.7
hexanes	3.84	17.2
heptenes	1.31	1
heptanes	2.44	2.6
heavier products	5.97	na
residue	2.73	na
total	99.99	99.403

[a] na = not available.

As an example, for pure butane at 200 °C and 1000 atm of pressure, the compressibility factor is about 2.6. Therefore, the real gas density is only about 38% of that predicted for an ideal gas. It was found that neglecting the deviation of the density from ideal gas behavior could cause dramatic changes in the overall rates of pyrolysis at high pressures, particularly at lower temperatures, but that the distribution of products was qualitatively similar.

Problem solutions (without sensitivity analysis) took from about 180 min for simulations at high temperatures (600 °C) to about 700 min for those at low temperatures (200 °C), where the problems are especially stiff, with reaction times of the order of 10^{14} s (tens of millions of years). No complete solutions with sensitivities were completed due to very large computation times on the workstations; rather, a few selected problems were restarted at reaction times of interest and allowed to run for relatively short periods of reaction time. Solutions in these cases still required on the order of 10^3 min of computer time due, in significant part, to the limitations of the system memory. These cases were selected to help provide confirmation of the major reaction pathways.

Results and Discussion

The problems of this study were solved as constant-temperature, constant-pressure problems. It should be noted that most pyrolysis experiments are conducted under constant-volume conditions, thus limiting quantitative comparisons. Initial simulations were conducted at high temperatures in order to examine the agreement between the present model and the existing database for pyrolysis of paraffins.

An initial comparison of the role of pressure may be made with the data of Hepp and Frey (1953). In essentially the only high-pressure study with relatively detailed product distribution data, they studied *n*-butane pyrolysis at 550 °C and at 160 atm of pressure in a tubular flow reactor system. Table I compares their results with those from the present model at an equivalent conversion level. The reaction time denotes, for Hepp and Frey's system, the "exposure time", and it is not made clear how this is defined or evaluated. For the present simulations, the reaction is based on a batch reactor model. That these times are rather different for the same level of butane conversion may be due to several factors. In the case of

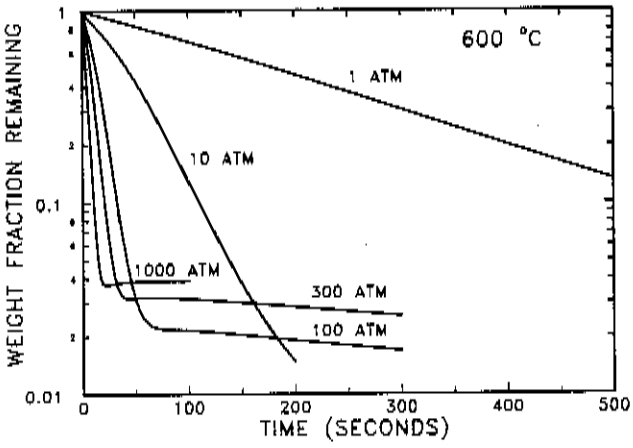

Figure 1. Butane decomposition rates at various pressures at 600 °C.

a tubular reactor where the number of moles increase significantly with increasing levels of conversion, the volumetric flow rate and gas velocity increase through the reactor which causes the actual time a volume element spends in the reactor to decrease from what is expected on the basis of inlet conditions. Additionally, thermal uniformity and the radial velocity distribution may contribute to uncertainty in the exposure time provided by Hepp and Frey. For the most part, the simulation results qualitatively agree well with the data. For example, H_2 is predicted to be a negligible reaction product, and alkane yields are significantly greater than olefin yields. The only major error in the model calculations is the overprediction in the yield of hexanes, which was traced to the truncation of the reaction mechanism model with species of seven carbon atoms. The accumulation of species with six carbon atoms occurs because addition reactions with two carbon species are a primary addition pathway. With butane as the fuel, there are high concentrations of C_4 radicals which would be expected to react together to produce C_8 species. Since C_8 species were not included in the reaction mechanism, these radicals instead lead to C_6 species. Since this is a transient effect, it is not expected to influence the long time solutions of the other problems addressed in this study.

At 600 °C, the rate of *n*-butane cracking is accelerated by increasing pressures, as shown in Figure 1, plotted on a weight basis. (It is more convenient to use a weight basis because the changing number of moles in the system makes mole fractions or molar concentrations a somewhat ambiguous relative measure.) This acceleration of the rate is in agreement with the literature, although, as mentioned above, there is little data beyond about 20 atm of pressure. The rate of decomposition at atmospheric pressure is in the range expected at this temperature (Fabuss et al., 1964), on the basis of a first-order process ($k = 3.6 \times 10^{-3}$ s^{-1}). It should be noted that there appears to be some deviation from linearity at the lower three pressures, but there does not appear to be an induction period even at the highest pressures. The equilibrium concentration of butane also increases with increasing pressure. This is in agreement with the literature (cf. Fabuss et al., 1964), which indicates increasing concentrations of higher molecular weight materials as pressure is increased. Although not shown on the figure, the lower pressure simulations eventually reach an equilibrium value of less than 1 wt % of the mixture.

The product distributions for simulations at atmospheric pressure, at 600 °C, are shown in Figures 2 and 3. The predominant products, shown in Figure 2, are ethylene and

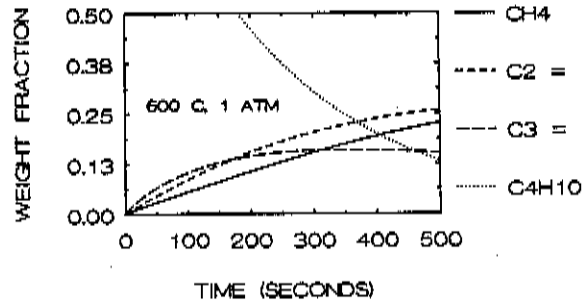

Figure 2. Butane decomposition and major products at 600 °C and 1 atm.

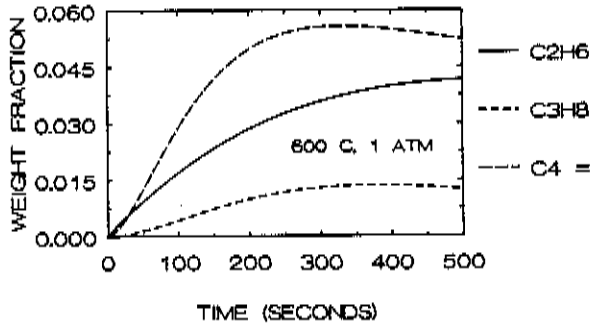

Figure 3. Light products of butane decomposition at 600 °C and 1 atm.

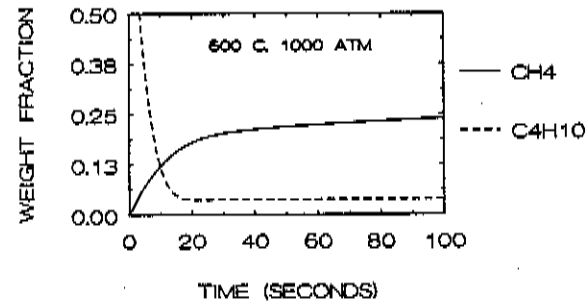

Figure 4. Butane decomposition and methane production at 600 °C and 1000 atm.

acetylene (shown togther as C2=, which is predominantly acetylene in this case) and methane, with propylene at a somewhat lesser value. Propylene shows the largest initial rate and a maximum concentration before butane becomes substantially depleted, thus appearing to be a significant primary product which undergoes a relatively slow secondary decomposition. Neither methane nor ethylene shows signs of induction and they therefore also appear to be primary products, although at slower initial rates of formation. At lower concentrations, four-carbon olefins, including butenes (primarily the α-olefin) and butadiene, show a slight induction period, while the light alkanes ethane and propane account for less than 6 wt % of the mixture. Although ethane shows no induction period, propane exhibits a pronounced one. All of the induction periods noted occur only at very low conversions and would appear to be related to the establishment of a steady radical population. No other products, and in particular those larger than four carbons, appear in other than very small amounts at this pressure. All of these results are in agreement with the literature under these reaction conditions.

At 600 °C and 1000 atm of pressure, the distribution of significant products is much broader, also in general agreement with the literature. These results are shown in Figures 4–6. Figure 4 shows that methane is the final product with the highest concentration, with a small in-

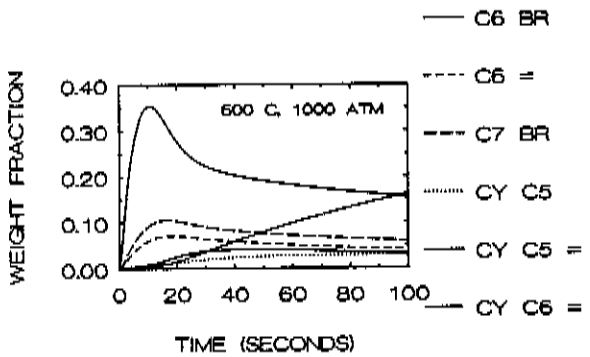

Figure 5. Heavy products of butane decomposition at 600 °C and 1000 atm.

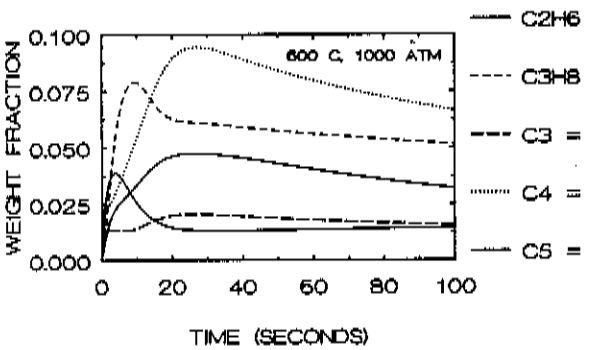

Figure 6. Light products of butane decomposition at 600 °C and 1000 atm.

duction period at very low conversion of the butane. The methane concentration continues to increase well after the butane concentration has achieved a steady concentration, indicative of production from secondary decomposition reactions. The dynamic behavior of the product distribution which occurs between 10 and 20 s of reaction time, concomitant with the depletion of butane, shown in Figures 5 and 6, is quite interesting. The largest transient species are the branched hexane isomers (denoted C6 BR), which show a very large maximum before achieving a slow rate of decomposition on a longer time scale. Examination of the products points to the addition reaction between ethyl and C4 olefins as the dominant reaction leading to formation of the branched C6s. It may be seen that ethane and the C4 olefins have very high initial rates of formation, with ethane's rate of decomposition quickly exceeding the formation rate at about 5 s of reaction time. The C4 olefins show a distinct slowing of their formation rate at the same time, with decomposition exceeding production at about the time that butane comes to its steady value. Propane shows behavior similar to ethane, but at a higher concentration and on a slightly longer time scale, evidently driving the production of C7 branched species. Branched C5 species are not significant products due to the much slower addition rate with methane. In all three cases, the presence of methane, ethane, and propane is indicative of the presence of the corresponding alkyl radicals, which are the reactive species in the addition reactions. Along with paraffinic species of all carbon numbers, the corresponding olefins are also present in significant, but not predominant, amounts. Ethylene is notable by its absence as a significant product at this pressure. Lastly, the presence of the larger species drives the secondary formation of cyclopentyl and cyclohexyl species.

As a summary of the results at 600 °C, Figure 7 illustrates the change in the molar carbon number distribution at three of the pressures studied. The major broadening of the distribution occurs at reaction pressures lower than

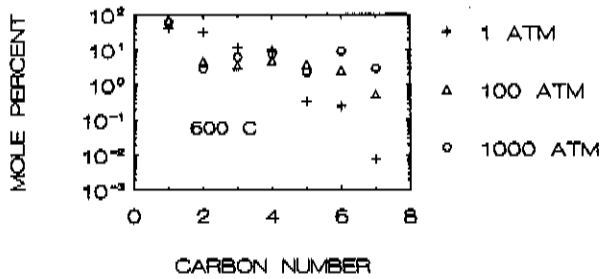

Figure 7. Effect of pressure on carbon chain size distribution at 600 °C.

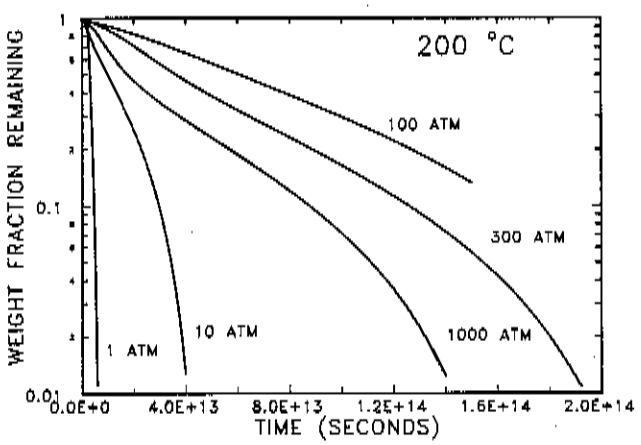

Figure 8. Butane decomposition rates at various pressures at 200 °C.

Table II. Comparison of Product Selectivities at High Butane Conversions at 600 and 200 °C (Molar Basis)

temperature	1 atm	100 atm	1000 atm
	Olefin Content/%		
200	3	1	1
600	43	29	20
	Branched Alkanes Content/%		
200	34	41	44
600	0	2	14
	n-Alkanes Content (Includes CH_4, C_2H_6, and C_3H_8)/%		
200	62	58	55
600	57	69	66

100 atm. Table II shows the fraction of the products at the end of a simulation, when all dynamics have died out, appearing as olefins, branched species, and normal alkanes, with all carbon numbers combined. The major observation is the reduction of the olefins content from 43 wt % of the product mixture at 1 atm to 20 wt % at 1000 atm. This reduction appears to occur continuously over the range of pressures, in contrast to the behavior of the carbon chain distribution. It is important to note that, with pure *n*-butane as the initial reactant, the hydrogen to carbon ratio of the system is fixed and therefore the amount of cracking to smaller products, requiring hydrogen, must be balanced by a source of hydrogen. In this case the source is either production of olefins or addition reactions. As the pressure increases, the reaction selectivity shifts to addition reactions, forming larger products, and therefore reduces the requirements of olefins production as the source of hydrogen. From the mechanistic standpoint at this temperature, there is a large radical pool created by unimolecular decomposition reactions. The high radical concentrations drive reactions of the alkyl (predominantly butyl) radicals. As the pressure increases, bimolecular reactions (hydrogen transfer) assume a relatively larger role providing a broader distribution of carbon numbers, which

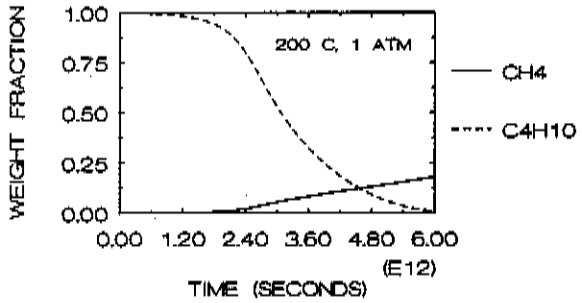

Figure 9. Butane decomposition and methane production at 200 °C and 1 atm.

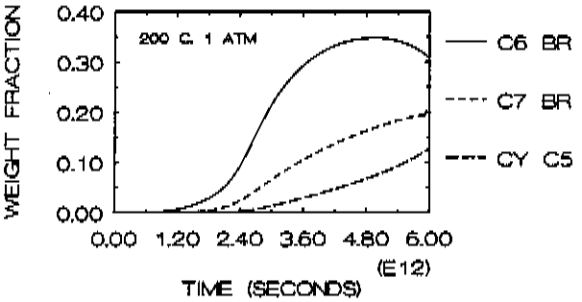

Figure 10. Heavy products of butane decomposition at 200 °C and 1 atm.

decreases the olefins content due to the fixed hydrogen to carbon ratio in the system.

At low temperature, 200 °C, the effect of pressure on the rate of decomposition of *n*-butane is reversed from that observed at high temperature. As may be seen in Figure 8, the rate is significantly slower as pressure is increased from 1 to 100 atm. Note that the time scale for this figure extends to 2×10^{14} s, or about 6.3×10^6 years. These extremely long reaction times explain the absence of experimental studies which cover the entire reaction history to high conversion at these low temperatures. The few studies in the literature at somewhat higher temperatures (ca. 300 °C) are therefore able to examine only the very earliest phases of the reactions, which may or may not reflect the longer time scale behavior of the system. This is therefore a strong motivation for the present type of computational analysis.

Above 100 atm the rate begins to increase. The reversal of the pressure effect is evidently, at least in part, due to the dampening of the increase in density with increasing pressure because of the compressibility factor in this pressure range, which is increasing approximately linearly with increasing pressure. This reversal of the effect of pressure on the rate begins to be apparent in the temperature range of 350–400 °C. In this range the rates of decomposition curves for each pressure cross at differing levels of butane conversion. One observation which presents itself, based upon the simulation results, is that data at low temperatures over small ranges of conversion may not reliably demonstrate the pressure dependence of the rate. This may be the reason that, for whole crude oils, McNab et al. (1952) saw no pressure dependence in the 310–370 °C temperature range. In contrast, Dominé (1989) found that, at the low conversions of his experimental study, the rate of decomposition of hexane was inhibited by increasing pressures at 357 °C. Also noticeable in Figure 8 is that the rates at all five pressures show significant deviation from first-order behavior with increasing rates of decomposition at high conversions of butane.

Figure 9 expands the time scale for the results at 200 °C and 1 atm to show the initial self-inhibition of the decomposition, as well as the delay in methane production.

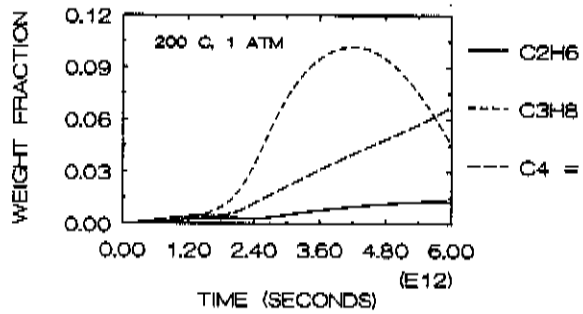

Figure 11. Light products of butane decomposition at 200 °C and 1 atm.

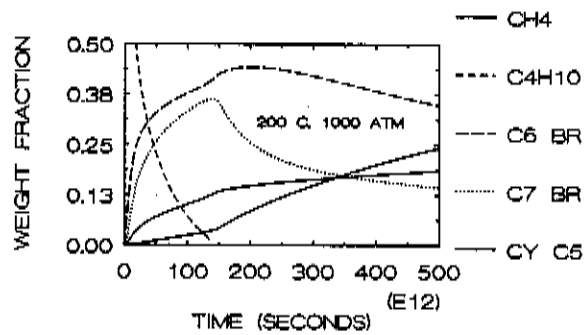

Figure 12. Butane decomposition and major products at 200 °C and 1000 atm.

The methane rate of formation appears to be zero order at longer reaction times, even after butane is depleted. Methane is still a predominant product, but the rate of production of branched C6 species, shown in Figure 10, exceeds that for methane, and from significantly earlier reaction times. Branched C7 species are also a significant product, although their appearance lags behind that of the C6 branched species. Also shown on this figure are the cyclic C5 species, which include methyl-, dimethyl-, and ethylcyclopentyl species. These are formed substantially from olefinic branched C6 and C7 species, and their rate of formation (by cyclization) shows an induction period lagging behind the appearance of the parent noncyclic species. Lastly, Figure 11 shows the primary light products with ethane and propane evidently driving the formation of the C6 and C7 species. The C4 olefins, almost entirely butadiene, exhibit zero-order behavior, even with butane almost completely depleted. Evidently, as butane becomes depleted, the addition–decomposition reaction forming the branched C6 species, which is initially driven in the addition direction, begins to shift toward the decomposition direction, thereby producing C4 olefins and depleting the branched C6 species. It should also be noted that ethylene is present only in trace quantities at these reaction conditions. The results for 1 atm at 200 °C are significantly different than those at high temperature. The product distribution is much broader in carbon number, and the olefins content is essentially eliminated at 200 °C, as may be noted in Table II.

At low temperature and high pressure, 1000 atm, markedly different dynamics in the product distribution appear as butane becomes depleted. This is shown in Figure 12. Methane is still a significant product, but the C6 and C7 branched species are the primary products at these conditions. As the butane becomes depleted at about 1.5×10^{14} s, the branched C7 species show a sudden increase in the rate of formation followed by a slow, approximately zero-order rate of loss after about 2.0×10^{14} s. The C7 branched species show a significant rate of decomposition upon depletion of the butane, while the

formation rate of the cyclic C5s shows an approximately equal rate of increase. Indeed, the primary C5 cyclics are predominantly seven-carbon species produced from the loss of C7 branched species and the balance from the C6 branched species. Aside from methane, the concentrations of other light species are quite low, with ethane achieving a maximum concentration of about 5.5 wt % at a reaction time of 1.5×10^{13} s before rapidly declining to a few tenths of a percent at the end of the simulation. Propane shows a similar behavior, with a maximum concentration of about 6.5 wt % at a reaction time of 8×10^{13} s and then a decline to a few tenths of a percent.

In comparing the low- and high-pressure results at 200 °C, there is a distinct shift to larger products with an essentially complete absence of light products other than methane. In Table II, it may be seen that there is an almost complete absence of olefins at all pressures. The ratio of normal to branched paraffins is also reduced with the increase in pressure. Mechanistically, at a relatively low temperature of 200 °C, the activation energy provides a large barrier to unimolecular decomposition, while recombination reactions, with no activation energy, play a larger role. These two factors produce the result of a relatively radical starved system. The large induction periods in the rate of butane decomposition are one indicator of this fact. As pressure is increased, the relative importance of recombination reactions increases as these become more effective.

Summary and Conclusions

At high pyrolysis temperatures, 600 °C, the effect of increasing pressure increases the decomposition rate of butane and decreases the olefins content while broadening the size distribution of the products. All of these results agree well with the knowledge base at these conditions. The inclusion of a relatively simple model for production of cyclic species provides results which seem to make intuitive sense, but there are little data available in the literature to confirm the validity of this part of the model.

At low temperatures, 200 °C, at the high end of the range of interest for geochemical studies, the results are significantly different, with increasing pressure generally decreasing the rate of decomposition with a diminishing effect at high pressures, above 100 atm. There are some data at moderate temperatures which support these results, but a more extensive database over a range of conversion levels is needed to validate these conclusions. A product distribution weighted toward larger products is also seen with increasing pressure, along with significant decreases in olefins content. The changes in selectivity are much more sensitive to the pressure and to the depletion of a dominant radical species (butyl) than at high temperatures.

Mechanistically, the differences between high- and low-temperature trends can best be understood in terms of the competitive reaction paths for alkyl and other large radical species. At the higher temperatures, radical decomposition is quite rapid and leads to a wide range of smaller molecular weight species, including chain-propagating radicals. Concentrations and collision rates among reactants increase with increasing pressure, and both the overall rate of reaction and the size distribution of the products increase. At the lower temperatures, however, the high activation energy barriers to alkyl decomposition reactions inhibit these reactions. Instead, radical species recombine, producing larger stable species and providing chain termination. As the pressure is increased at these lower temperatures, the rates of recombination processes also increase, further decreasing the overall rate of decomposition.

Even though the kinetic model used here omits potentially important effects of minerals, heteroatoms, labile hydrogen donors, carbon residue, and organometallics that would be present in most real subsurface petroleum environments, our results clearly indicate that the extrapolation of the pressure dependence of other pyrolysis models from high to low temperatures may be substantially in error. It is significant that the basic conclusion that pressure accelerates cracking at high temperature and inhibits cracking at low temperature was observed throughout many adaptations of the mechanism during the course of this study. Even so, confirmation of these results at experimentally feasible low temperatures would be of great value. The application of the results of this model may be seen in better understanding petroleum maturation processes as well as chemical processing under high pressure and moderate temperature conditions, such as those used for oil shale and coal liquefaction processing.

Acknowledgment

This work was performed under the auspices of the U.S. Department of Energy by Lawrence Livermore National Laboratory under Contract No. W-7405-ENG-48. R.G.M. is grateful to The Associated Western Universities for support from a Faculty Sabbatical Fellowship. We are also indebted to F. M. Rupley, A. E. Lutz, and R. J. Kee of Sandia National Laboratory, Albuquerque, NM, for assistance in implementation of the CHEMKIN-II software.

Registry No. C_4H_{10}, 106-97-8.

Literature Cited

Allara, D. L.; Shaw, R. J. A Compilation of Kinetic Parameters for the Thermal Degradation of *n*-Alkane Molecules. *J. Phys. Chem. Ref. Data* **1980**, *9*, 523.

Asano, T.; Le Noble, W. J. Activation and Reaction Volumes in Solution. *Chem. Rev.* **1978**, *78*, 407.

Axelsson, E. I.; Brezinsky, K.; Dryer, F. L.; Pitz, W. J.; Westbrook, C. K. Chemical Kinetic Modeling of The Oxidation of Large Alkane Fuels: *n*-Octane and Isooctane. *Twenty-first Symposium (International) on Combustion.* The Combustion Institute: Pittsburgh, PA, 1986; pp 783–793.

Benson, S. W. *Thermochemical Kinetics*, 2nd ed.; Wiley Interscience: New York, 1976.

Caracotsios, M.; Stewart, W. E. Sensitivity Analysis of Initial Value Problems Including ODE's and Algebraic Equations. *Comput. Chem. Eng.* **1985**, *4*, 359.

Dominé, F. Kinetics of Hexane Pyrolysis at Very High Pressures. 1. Experimental Study. *Energy Fuels* **1989**, *3*, 89.

Dominé, F. High Pressure Pyrolysis of *n*-Hexane, 2,4-Dimethylpentane and 1-Phenylbutane. Is Pressure an Important Geochemical Parameter? *Org. Geochem.* **1991**, in press.

Dominé, F.; Marquaire, P.-M.; Muller, C.; Côme, G.-M. Kinetics of Hexane Pyrolysis at Very High Pressures. 2. Computer Modeling. *Energy Fuels* **1990**, *4*, 2.

Doue, F.; Guiochon, G. The Formation of Alkanes in the Pyrolysis of *n*-Hexadecane: Effect of an Inert Gas on the Decomposition of Alkyl Radicals. *J. Chim. Phys. Phys.-Chim. Biol.* **1968**, *65*, 3477.

Ebert, K. H.; Ederer, H. J.; Stabel, U. *Pyrolysis Up To High Degrees of Conversion*; Universität Heidelberg: Heidelberg, Germany, 1983; SFB 123, Number 225.

Fabuss, B. M.; Smith, J. O.; Satterfield, C. N. Thermal Cracking of Pure Saturated Hydrocarbons. *Adv. Pet. Chem. Refin.* **1964**, *9*, 157.

Gonikberg, M. G.; Gavrilova, A. E.; Kazanskii, B. A. The Thermal and Catalytic Cracking of Paraffinic Hydrocarbons Under High Pressures. *Dokl. Akad. Nauk SSSR* **1953**, *89*, 483.

Hepp, H. J.; Frey, F. E. Pyrolysis of Propane and Butanes at Elevated Pressure. *Ind. Eng. Chem.* **1953**, *45*, 410.

Kee, R. J.; Rupley, F. M.; Miller, J. A. CHEMKIN-II: A Fortran Chemical Kinetics Package for the Analysis of Gas-Phase Chemical Kinetics; Sandia National Laboratories Report SAND89-8009;

Sandia National Laboratories: Albuquerque, NM, 1989.
Kossiakoff, A.; Rice, F. O. Thermal Decomposition of Hydrocarbons, Resonance Stabilization and Isomerization of Free Radicals. *J. Am. Chem. Soc.* **1943**, *65*, 590.
Lutz, A. E.; Kee, R. J.; Miller, J. A. SENKIN: A Fortran Program for Predicting Homogeneous Gas-Phase Chemical Kinetics with Sensitivity Analysis. Sandia National Laboratories Report SAND87-8248; Sandia National Laboratories: Albuquerque, NM, 1987.
McNab, J. G.; Smith, P. V., Jr.; Betts, R. L. The Evolution of Petroleum. *Ind. Eng. Chem.* **1952**, *44*, 2556.
Rice, F. O.; Herzfeld, K. F. The Thermal Decomposition of Organic Compounds from the Standpoint of Free Radicals. VI. The Mechanism of Some Chain Reactions. *J. Am. Chem. Soc.* **1934**, *56*, 284.
Starling, K. E.; Kumar, K. H. Computer Program for Natural Gas Supercompressibility Factor, Custody Transfer Calculations and Process Calculations Using the OU/GRI Correlation. *Preprints of the 64th Annual Gas Processors Convention*, Houston, TX; Gas Processors Association: Tulsa, OK, 1985.
Stull, D. R.; Westrum, E. F., Jr.; Sinke, G. C. *The Chemical Thermodynamics of Organic Compounds*; Kreiger: Malabar, FL, 1987.
Voge, H. H.; Good, G. M. Thermal Cracking of Higher Paraffins. *J. Am. Chem. Soc.* **1949**, *71*, 593.
Westbrook, C. K.; Warnatz, J.; Pitz, W. J. A Detailed Chemical Kinetics Reaction Mechanism for the Oxidation of Isooctane and *n*-Heptane Over an Extended Temperature Range and Its Application to Analysis of Engine Knock. *Twenty-second Symposium (International) on Combustion*; The Combustion Institute: Pittsburgh, PA, 1988; pp 893–901.

Received for review April 1, 1991
Revised manuscript received August 8, 1991
Accepted August 22, 1991